Z. Phys. C - Particles and Fields 52, 231–238 (1991)

Zeitschrift für Physik C Particles and Fields

Deuteron production in collisions of 250 GeV/c π^+ and K^+ mesons with Al and Au nuclei

EHS-NA22 Collaboration

N.M. Agababyan[1], H. Boettcher[2], F. Botterweck[3], M.M. Chapkin[4], M. Charlet [3, a], P.V. Chliapnikov[4], A. De Roeck[5, b], E.A. De Wolf[5, c], K. Dziunikowska[6*], G. Gulkanyan[1], T. Haupt[3, d], K. Kaleba[6*], W. Kittel[3], A.B. Michalowska[5], K. Olkiewicz[6*], F.K. Rizatdinova[7], E.K. Shabalina[7], O.G. Tchikilev[4], V.A. Uvarov[4], F. Verbeure[5]

[1] Institute of Physics, SU-375036 Yerevan, USSR
[2] Institut für Hochenergiephyisik O-1615 Berlin-Zeuthen, Federal Republic of Germany
[3] University of Nijmegen and NIKHEF-H, NL-6525 ED Nijmegen, The Netherlands
[4] Institute for High Energy Physics, SU-142284 Serpukhov, USSR
[5] Dept. of Physcis, Universitaire Instelling Antwerpen, B-2610 Wilrijk, and Interuniversity Institute for High Energies, B-1050 Brussels, Belgium
[6] Institute of Physics and Nuclear Techniques of the Academy of Mining and Metallurgy and Institute of Nuclear Physics, PL-30055 Krakow, Poland
[7] Moscow State University, SU-119899 Moscow, USSR

Received 21 January 1991; in revised form 18 June 1991

Abstract. Experimental data are presented on deuteron production in the target fragmentation region for 250 GeV/c π^+ and K^+ interactions with Al and Au nuclei, and compared with analogous data on proton production. Indications are observed for narrow structures in the $(d\pi^-)$ effective mass system at $\sim$2.04 and $\sim$2.08 GeV.

1 Introduction

Composite fragments are copiously produced in interactions of high energy hadrons with nuclei. The study of this production is equally important for the understanding of nuclear structure as of particle production mechanisms. Many different production mechanisms (direct knock-on of preformed deuteron-like clusters, pick-up processes, the tail of evaporation, coalescence, etc.) exist and complicate the analyses of the data on production of the lightest fragment, the deuteron. For a review of the data and models see [1a, 2, 3]. Experimental data mainly exist for proton beams, either from emulsion experiments (which suffer from low statistics and unknown target nucleus [1b–d]) or from electronic experiments (which usually measure only momentum spectra at fixed laboratory angles).

Interest in deuteron production was revived [4] due to calculations showing that the ratio d/p of the deuteron to proton yields is connected to the entropy and, therefore, can be used in searches of the quark-gluon plasma. For a review of the subject of entropy production, see [3].

The interest in deuteron production is, furthermore, related to recent searches for narrow dibaryons (for reviews see [5]). Theoretical estimates indicate that the deuteron can have some six-quark state admixture [6–8].

The experimental status of narrow dibaryon searches is still rather controversial. For example, a recent LAMPF observation [9] of exotic states with charge -1 and $+3$ near 2 GeV with marginal statistical significance, has not been confirmed (for charge $+3$) by data from the SPECIII spectrometer at the Saturne accelerator [10]. Moreover, one needs to look for non-exotic states, since there exist theoretical predictions (for example in the model of elongated rotating $6q$ bags [11]) for isospin $I=0$ and $I=1$ states in addition to exotic $I=2$ states.

The aim of this paper is to present experimental data on a comparison of general characteristics of deuteron and proton production in collisions of 250 GeV/c π^+ and K^+ mesons with Al and Au nuclei and on the results of a search for narrow dibaryon states in $d\pi^-$ and $d\pi^+$ effective mass spectra.

---

[a] EEC Guest Scientist
[b] Onderzoeker IIKW, Brussels, Belgium, now at MPI, München, FRG
[c] Bevoegdverklaard Navorser NFWO, Belgium
[d] Now at Syracuse University, Syracuse NY 13244-1130, USA
* Partially supported by grants from CPBP 01.06 and 01.09

2 The data sample

The data derive from an experiment using the CERN European Hybrid Spectrometer (EHS), equipped with the Rapid Cycling Bubble Chamber (RCBC), filled with H_2 and serving as vertex and track detector as well as an ionization device. Two thin nuclear targets, one of aluminum and one of gold, are placed side by side orthogonally to the beam, 15.5 cm behind the entrance window of the chamber. Charged tracks, leaving the bubble chamber through the exit window, are measured in a two-lever arm spectrometer, consisting of seven wire or drift chambers, interspersed with charged particle identification devices, gamma-detectors and hadron calorimeters. A more detailed description of the set-up and minimum bias trigger used is given in [12, 13]. Previous results presented on this sample of events are on multiplicity distributions [13] and on rapidity and transverse momentum distributions [14].

In the present analysis, we only use events in which positive tracks with laboratory momentum $p_{\text{lab}} < 1.2$ GeV/c and negative tracks with $p_{\text{lab}} < 0.2$ GeV/c have been visually identified by ionization in RCBC. Events are required to have a well reconstructed vertex in the foil region, a well reconstructed beam track and at least one reconstructed secondary track. Badly reconstructed low energy tracks are discarded during the ionization scan. We have checked that the use of more stringent criteria of event selection [13–14], has little influence on the results presented here. Since we do not observe any significant difference between the π^+ and the K^+ sample within the limits of statistics, we present our data for the combined sample of π^+ and K^+ collisions, which we call "M^+" collisions, in order to enhance the statistical significance. The total number of events used is 4200 for M^+ Al interactions and 3700 for M^+ Au interactions.*

To correct for multiplicity dependent losses in the measurement and reconstruction procedure, we normalize the data sample used, separately for the Al and Au targets, to the charged particle multiplicity distribution observed at the measurement stage. The weight varies from ~ 1.2 at lower charged particle multiplicities to ~ 1.8 at $n_{\text{ch}} \sim 60$, practically linearly with multiplicity.

Tracks are accepted when $\Delta p/p < 30\,\%$. The momenta of particles, based on measurements in the hydrogen and/or the spectrometer, are corrected for ionization losses inside the foils. This correction is most significant for low energy particles, emitted at small angles with respect to the foils. The uncertainty in this correction is mainly related to the resolution in the vertex position measurement inside the foils and is larger for the Au than for the Al target.

The fiducial volume of RCBC is a cylinder with 40 cm radius and the depth along the cylinder axis is restricted to ± 18 cm. A 2T magnetic field is applied along the cylinder axis. We have full angular acceptance for stopping deuteron tracks in the forward hemisphere with $p_{\text{lab}} < 0.5$ GeV/c (corresponding to a track length less than 18 cm). For tracks with angle of emission $\vartheta < 45°$ with respect to the beam direction, this momentum range extends to ~ 0.6 GeV/c. In the backward hemisphere some tracks are stopped in the ring with fiducial crosses and, in general, the momentum resolution is worse because of optical distortions and foil shadows. We therefore only consider forward going deuterons.

* The number of K^+ events is about one third of the number of π^+ events. For part of the analysis, a larger sample of 5000 and 4300 events, respectively, was used

3 Deuteron multiplicities

To select deuterons, we apply the method used by the NA23 collaboration [15] in a study of a small sample of pA collisions at 360 GeV/c in the same experimental set-up. The method is based on the range-momentum relation and can be used for tracks with momentum measurement from the track curvature and range measurement from the endpoint in the liquid hydrogen of RCBC. The range l is characterized by a power dependence on laboratory momentum p, with the same exponent but different coefficient for different particle masses. Therefore, the linear combination of logarithms

$$R = 0.96194 \log_{10} p\,(\text{GeV}) - 0.27328 \log_{10} l\,(\text{cm}) \qquad (1)$$

can be used to discriminate between different masses. The variable R can be visualized as a measure perpendicular to the different range-momentum curves on a double-logarithmic plot (see the figure on page 69 in [16]). For accurately measured tracks, the R values for the mass hypotheses of interest are -0.82 (p), -0.61 (d), -0.50 (tritium) and -0.25 (α-particle).

The distribution of R for all forward going positive stopping tracks with a curvature measurements ($\Delta p/p < 0.3$) is shown in Fig. 1a. One observes a large peak due to stopping protons and a smaller deuteron peak. As expected*, there is no noticeable signal from tritons nor α-particles. The deuteron peak becomes more pronounced when requiring $p_{\text{curv}} > 0.35$ GeV/c (Fig. 1b), where stopping deuteron tracks have a range $l > 5$ cm.

To select deuterons, we therefore require $p_{\text{curv}} > 0.35$ GeV/c, the emission angle ϑ to be smaller than 90° and R to be in the interval

$$-0.69 < R < -0.53\,. \qquad (2)$$

To estimate the magnitude of the deuteron signal, we fit the R distribution to a sum of two gaussian distributions in 50 MeV/c wide intervals of momentum, starting from $p_{\text{lab}} = 0.35$ GeV/c. From these fits it appears that the proton admixture in the interval (2) decreases from 22 % for $0.35 < p_{\text{lab}} < 0.40$ GeV/c to a negligible level for $p_{\text{lab}} > 0.50$ GeV/c and we derive a momentum dependent correction factor which takes into account this proton admixture as well as the loss of deuterons in the tails of the R distribution.

In the following we present deuteron data selected by cut (2), corrected for geometrical inefficiencies connected

* Saniewska et al. [1 b] have observed a t/d ratio of about 5% in p interactions on heavy nuclei at 24 GeV/c

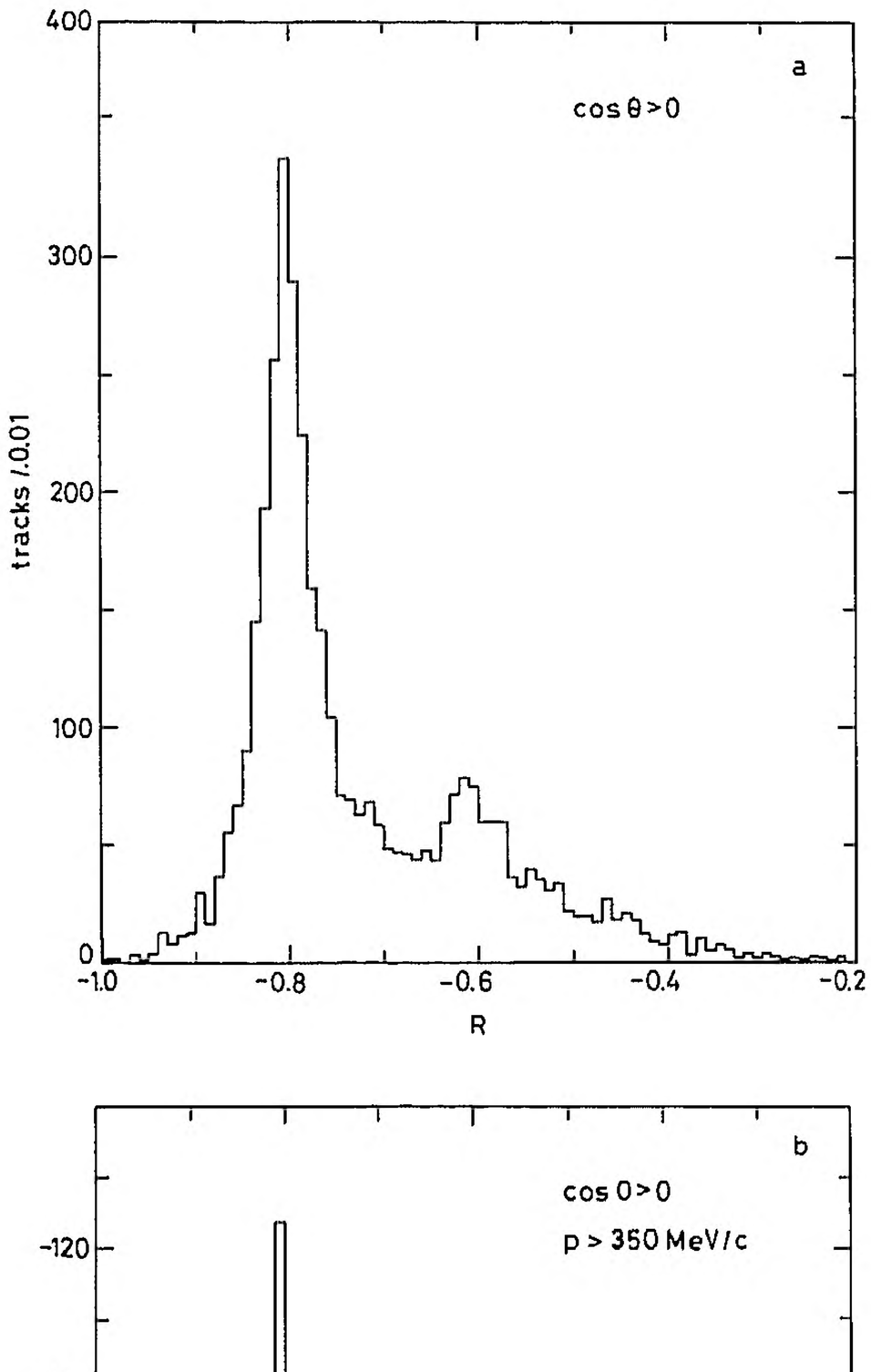

Fig. 1a, b. Distribution of R (see definition in the text) of forward emitted positive stopping tracks with $(\Delta p/p)_{\text{curv}} < 0.3$ for the combined sample of M^+Al and M^+Au events **a** for all tracks; **b** for tracks with $p_{\text{curv}} > 0.35$ GeV/c

with the restricted fiducial volume of the RCBC, and for the loss of deuterons which are emitted at small angles with respect to the foils, i.e. with ϑ close to 90°. The latter correction amounts to 3%. The momentum dependent correction for geometrical ineffeciencies is calculated as follows: each observed deuteron track is rotated around the beam direction and the stopping point is calculated, taking into account the magnetic field; the fraction of rotated tracks with stopping point inside the fiducial volume is used as a measure of the geometrical efficiency.

Table 1. Number of weighted events as a function of the number of forward produced deuterons n_d

n_d	Al		Au	
0	5907	±86	4916	±80
1	400	±31	1041	±57
2	23.7	±10.1	410	±57
3	–		54	±22
4	–		65	±36
5	–		54	±54
$\langle n_d \rangle$	0.071 ±	0.004	0.390 ±	0.013

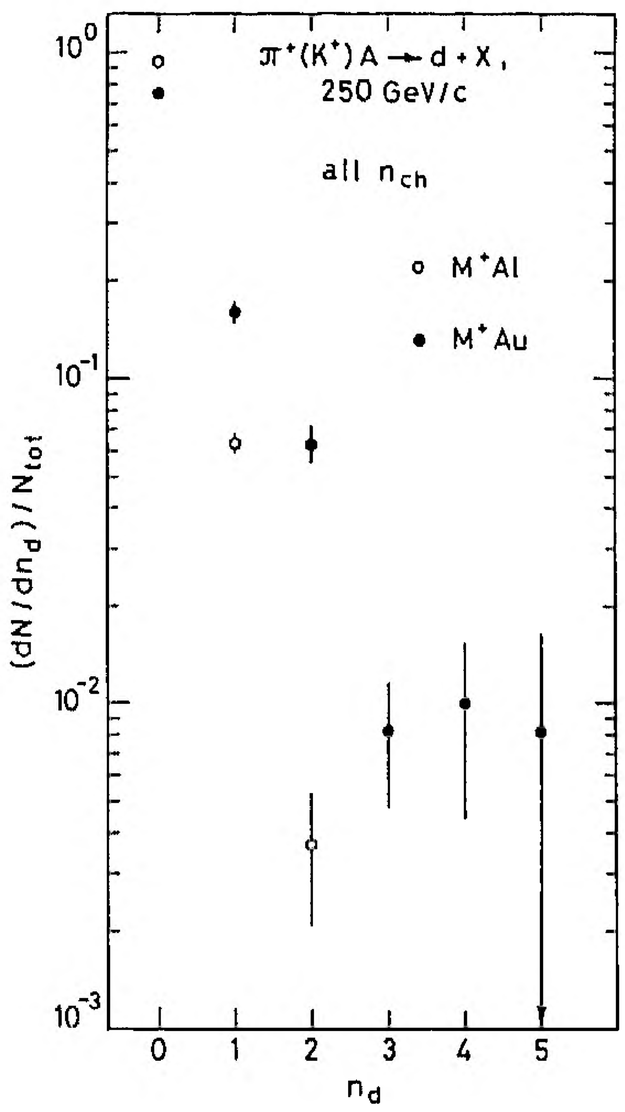

Fig. 2. Probability distribution of the number of produced deuterons for Al and Au trargets

Deuterons emitted at smaller angles wrt the beam, can have a longer range in the hydrogen of RCBC and their momentum can be measured with higher precision. Therefore, as a check of our results, we also use the following two kinematical regions:

$$\vartheta < 90° \quad \text{and} \quad 0.4 < p(d) < 0.5\ \text{GeV/c}, \tag{3}$$

and

$$\vartheta < 45° \quad \text{and} \quad 0.4 < p(d) < 0.6\ \text{GeV/c}. \tag{4}$$

The probability distribution of the number n_d of deuterons, selected according to (2), is given in Table 1 and shown in Fig. 2. The average number of deuterons per event, $\langle n_d \rangle$, is 0.071 ± 0.004 for M^+Al and 0.390 ± 0.013 for M^+Au interactions. This can be compared with the values 0.22 ± 0.13 and 0.65 ± 0.10, obtained respectively for pAl and pAu collisions at 360 GeV/c [15]. It thus appears that incident protons are more efficient in producing deuterons in nuclear collisions.

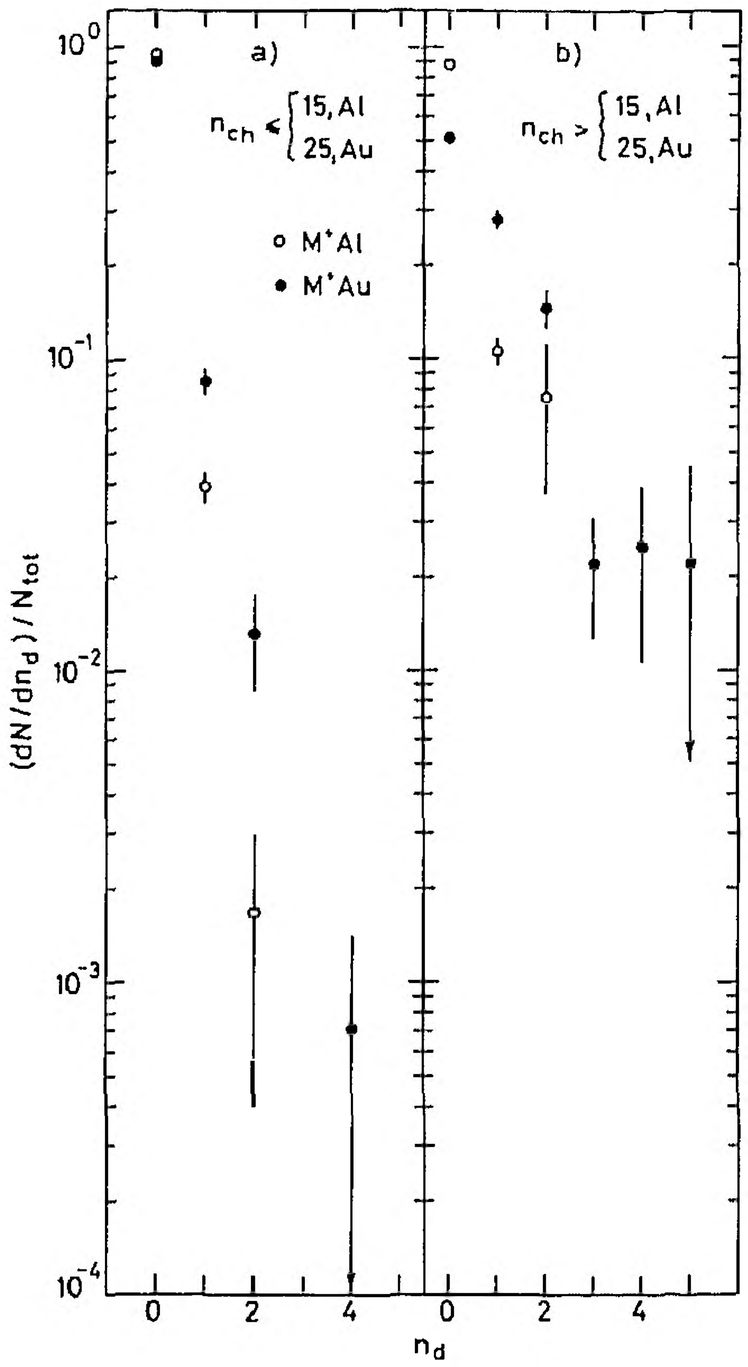

Fig. 3a, b. As in Fig. 2 for events with: **a** $n_{ch} \leqq 15$ (Al) or $\leqq 25$ (Au) **b** $n_{ch} < 15$ (Al) or > 25 (Au)

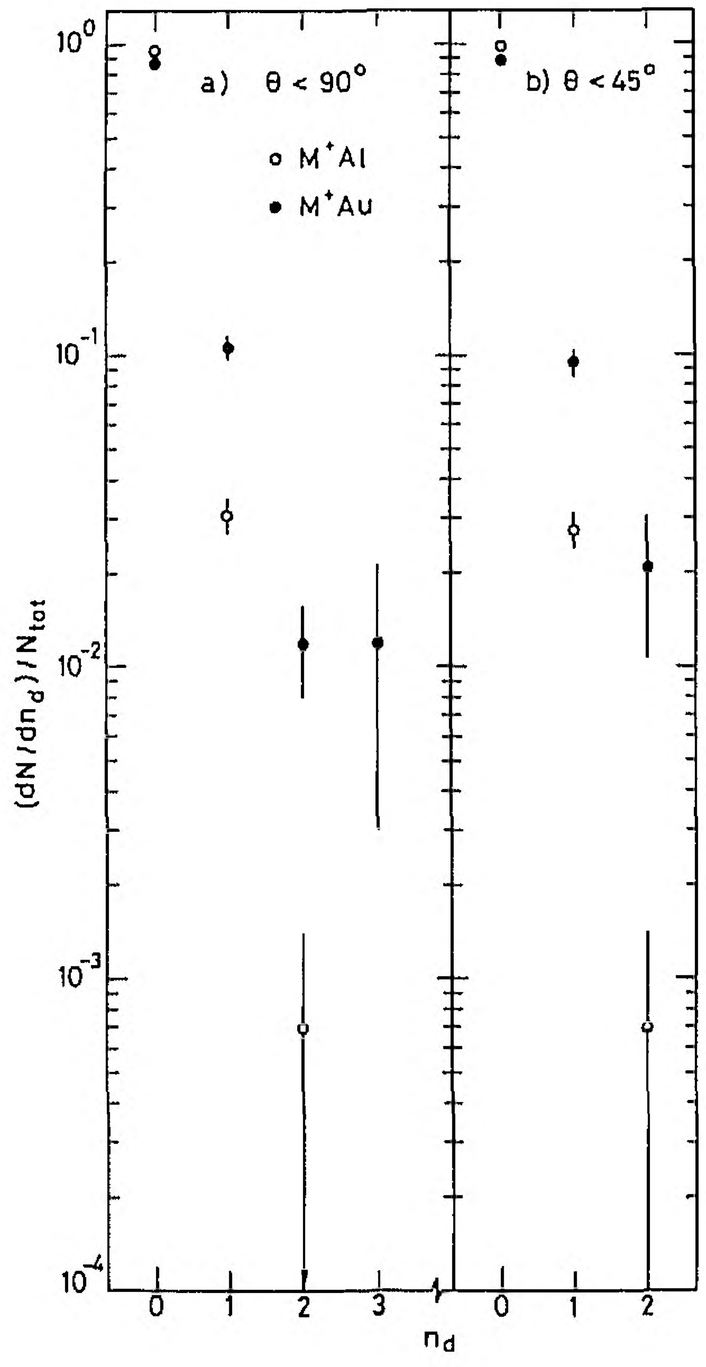

Fig. 4a, b. As in Fig. 2 with the following cuts on the deuteron: **a** $\vartheta < 90°$, $0.4 < p(d) < 0.5$ GeV/c; **b** $\vartheta < 45°$, $0.4 < p(d) < 0.6$ GeV/c

Table 2. As in Table 1, for forward ($\vartheta < 90°$) produced deuterons with $0.4 < p_{lab} < 0.5$ GeV/c

n_d	Al	Au
0	6130 ±89	5676 ±98
1	195 ±24	706 ±60
2	4.7 ± 4.7	78.2 ±32.3
3	–	80.2 ±60.0
$\langle n_d \rangle$	0.032 ± 0.003	0.169 ± 0.007

Table 3. As in Table 1, for deuterons with $\vartheta < 45°$, $0.4 < p < 0.6$ GeV/c

n_d	Al	Au
0	6153 ±89	5786 ±106
1	173 ±21	618 ± 51
2	4.7 ± 4.7	137 ± 67
$\langle n_d \rangle$	0.029 ± 0.002	0.136 ± 0.006

The number of events decreases exponentially with increasing n_d, with a larger slope for M^+Al than for M^+Au collisions. A similar exponential decrease is observed for low ($n_{ch} \leqq 15$ for Al, $n_{ch} \leqq 25$ for Au) and for high ($n_{ch} > 15$ (Al), $n_{ch} > 25$ (Au)) charge multiplicities (Fig. 3). The slope is smaller for high multiplicities and in all cases it is smaller for M^+Au than for M^+Al. The same effect is observed for the less biased n_d spectra (Tables 2 and 3 and Fig. 4), obtained using the cuts (3) and (4). We notice that the ratio of the average number of produced deuterons in Au to the one in Al is always about five, whatever selection is made (see Tables 1 to 3).

For comparison, the probability distribution of the number of protons with momentum

$$0.2 < p_{lab}(p) < 1.2 \text{ GeV/c}$$

is shown in Fig. 5a for low n_{ch} and in Fig. 5b for high n_{ch}. The lower cut on the proton momentum is necessary to avoid the region where very short stopping tracks are lost because of foil shadows. The upper cut corresponds to the limit of visual identification by ionization in RCBC. The distributions in Fig. 5 are considerably less biased than the d data, since geometrical inefficiencies are small and the admixture of deuterons in the proton sample is concentrated mainly at momenta below ~0.3 GeV/c. For small n_{ch}, the proton probability distributions also have an approximate exponential behavior with a smaller slope for the Au than for the Al target. At higher n_{ch} a dip at $n_p = 0$ is observed, but also there the exponential decrease at the larger n_p values is steeper for the Al than for the Au target.

The dependence of the average deuteron multiplicity $\langle n_d \rangle$ on n_{ch}, is given in Table 4 and Fig. 6. For $n_{ch} < 15$, $\langle n_d \rangle$ rises quadratically with n_{ch} and practically coincides for the Al and Au targets. At higher n_{ch}, it grows linearly with n_{ch} both in the Al and Au samples, but with a con-

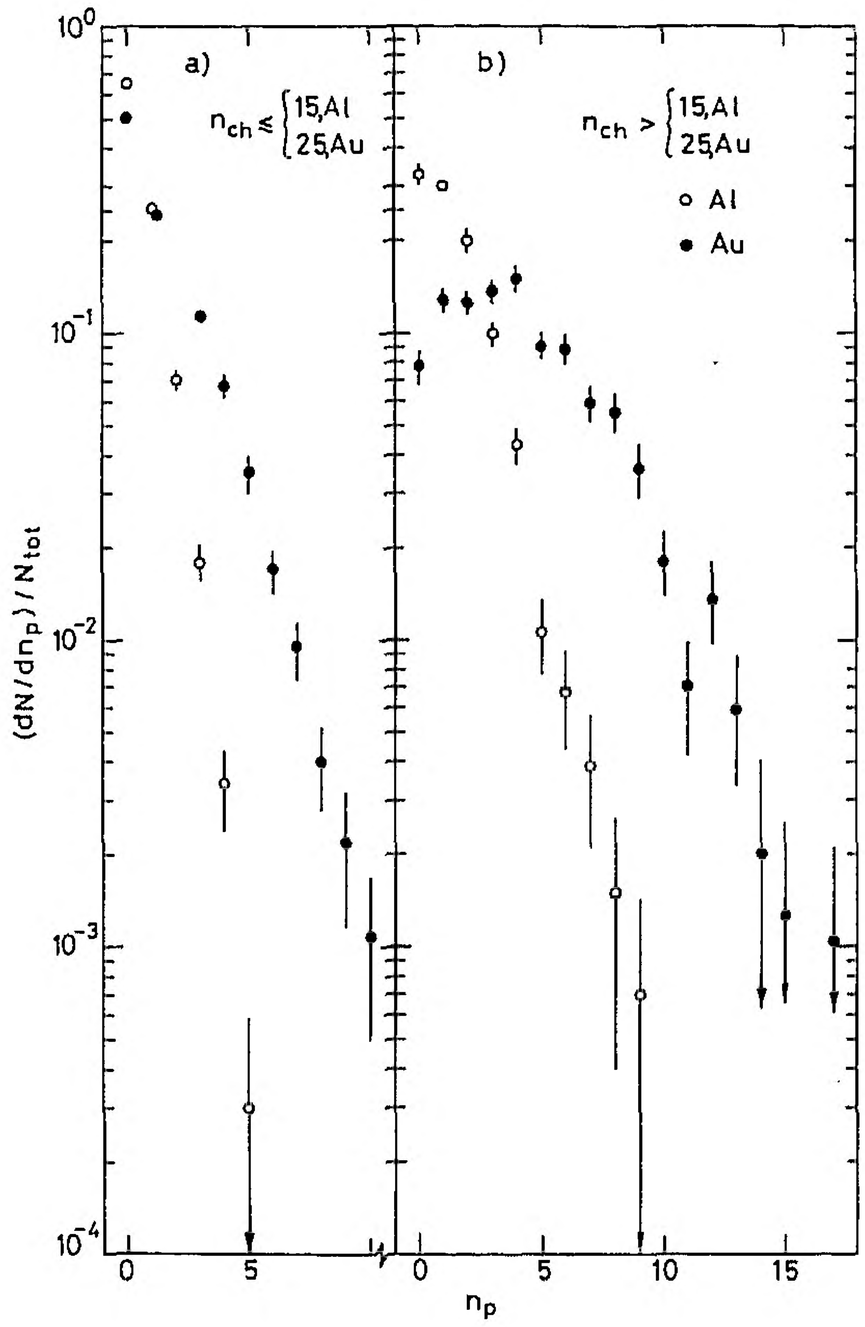

Fig. 5a, b. Probability distribution of the number of produced protons with $0.2 < p_{lab}(p) < 1.2$ GeV/c: **a** for $n_{ch} \leqq 15$ (Al), 25 (Au); **b** for $n_{ch} > 15$ (Al), 25 (Au)

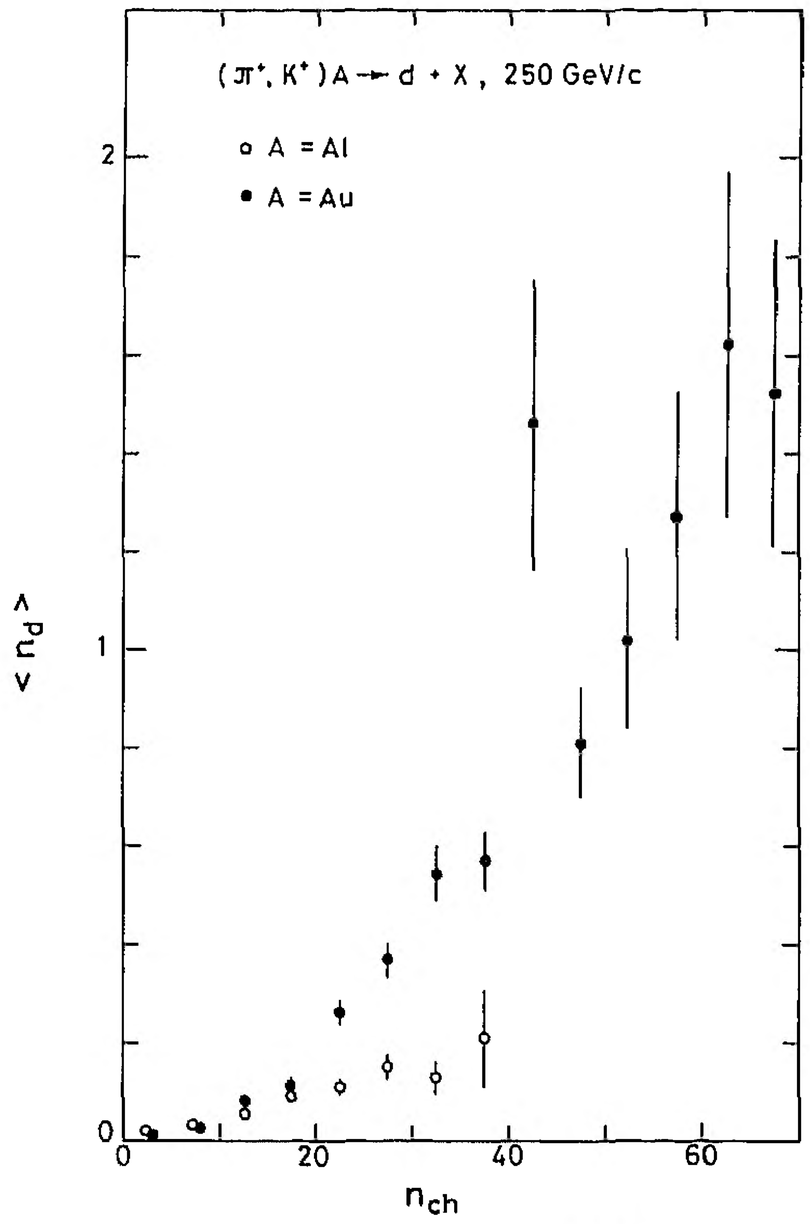

Fig. 6. Mean number of deuterons $\langle n_d \rangle$ as a function of charged particle multiplicity n_{ch}

Table 4. Average deuteron multiplicity $\langle n_d \rangle$ as a function of the charged particle multiplicity n_{ch}

n_{ch}-interval	Al	Au
1 ÷ 4	0.021 ± 0.007	0.013 ± 0.006
5 ÷ 9	0.034 ± 0.006	0.028 ± 0.007
10 ÷ 14	0.055 ± 0.006	0.085 ± 0.011
15 ÷ 19	0.089 ± 0.010	0.114 ± 0.013
20 ÷ 24	0.113 ± 0.015	0.266 ± 0.024
25 ÷ 29	0.152 ± 0.027	0.371 ± 0.037
30 ÷ 34	0.129 ± 0.036	0.546 ± 0.053
35 ÷ 39	0.214 ± 0.102	0.572 ± 0.063
40 ÷ 44	–	1.460 ± 0.290
45 ÷ 49	–	0.808 ± 0.116
50 ÷ 54	–	1.020 ± 0.180
55 ÷ 59	–	1.280 ± 0.250
60 ÷ 64	–	1.620 ± 0.350
65 ÷ 69	–	1.420 ± 0.310

siderably larger slope in the latter case. Practically the same behaviour is observed for $\langle n_d \rangle$ in the kinematical regions (3) and (4) (see Fig. 7).

The correlation between the average number of deuterons and the number of protons in an event, is given in Table 5 and shown in Fig. 8. For both the Al and Au targets, $\langle n_d \rangle$ rises linearly with n_p. This observation contradicts the behavior expected in the model of Butler and Pearson [17], yielding (at fixed momentum) a linear dependence of n_d on n_p^2.

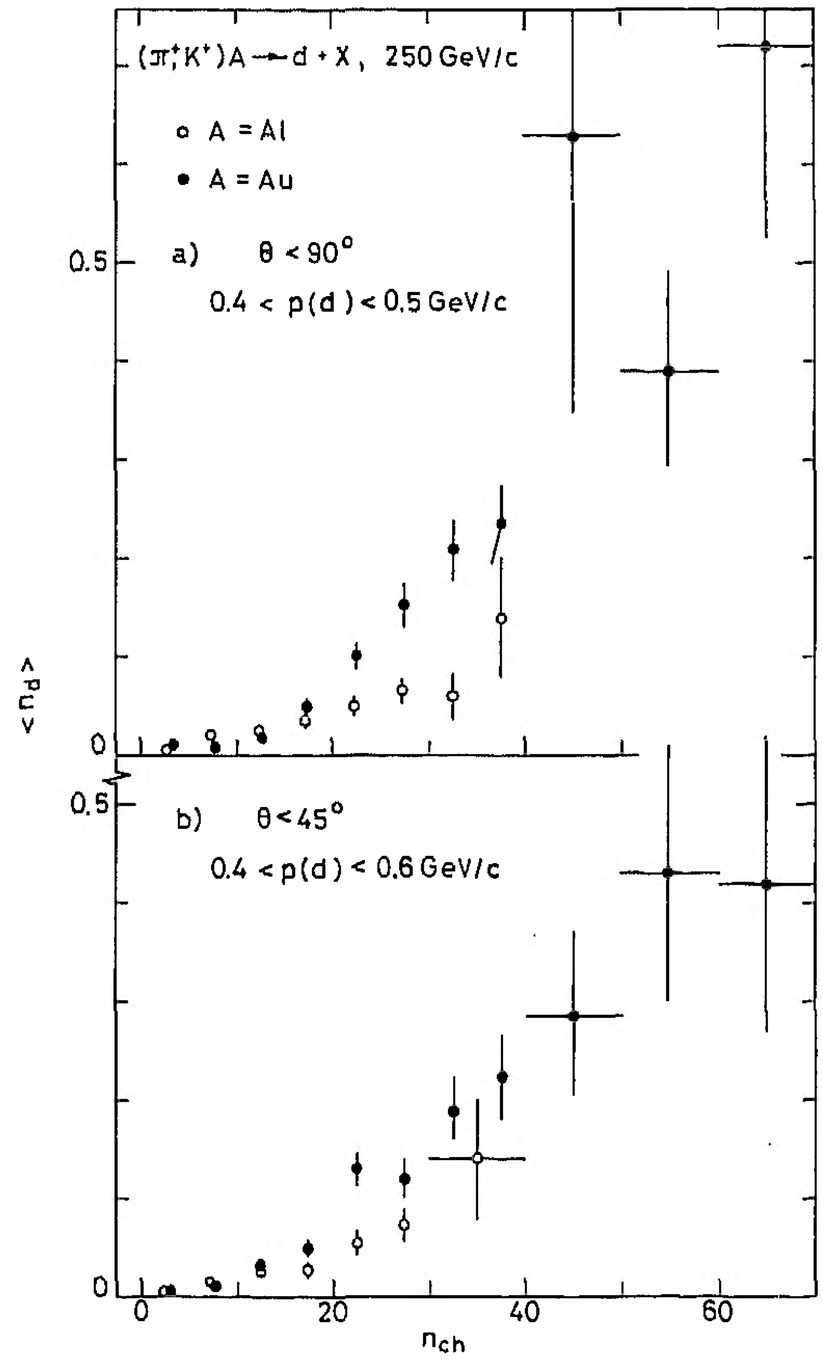

Fig. 7a, b. As in Fig. 6 with the following cuts on the deuteron: **a** $\vartheta < 90°$ and $0.4 < p(d) < 0.5$ GeV/c; **b** $\vartheta < 45°$ and $0.4 < p(d) < 0.6$ GeV/c

Table 5. Average multiplicity of deuterons $\langle n_d \rangle$ versus number of produced protons n_p

n_p	Al	Au
0	0.047 ± 0.005	0.073 ± 0.009
1	0.060 ± 0.007	0.164 ± 0.015
2	0.107 ± 0.015	0.263 ± 0.027
3	0.100 ± 0.022	0.337 ± 0.036
4	0.247 ± 0.063	1.020 ± 0.190
5	–	0.485 ± 0.065
6	–	0.985 ± 0.118
7	–	0.980 ± 0.166
$8 \div 9$	–	1.078 ± 0.211
$10 \div 11$	–	1.105 ± 0.223
$12 \div 13$	–	1.027 ± 0.245
$14 \div 15$	–	1.538 ± 0.353

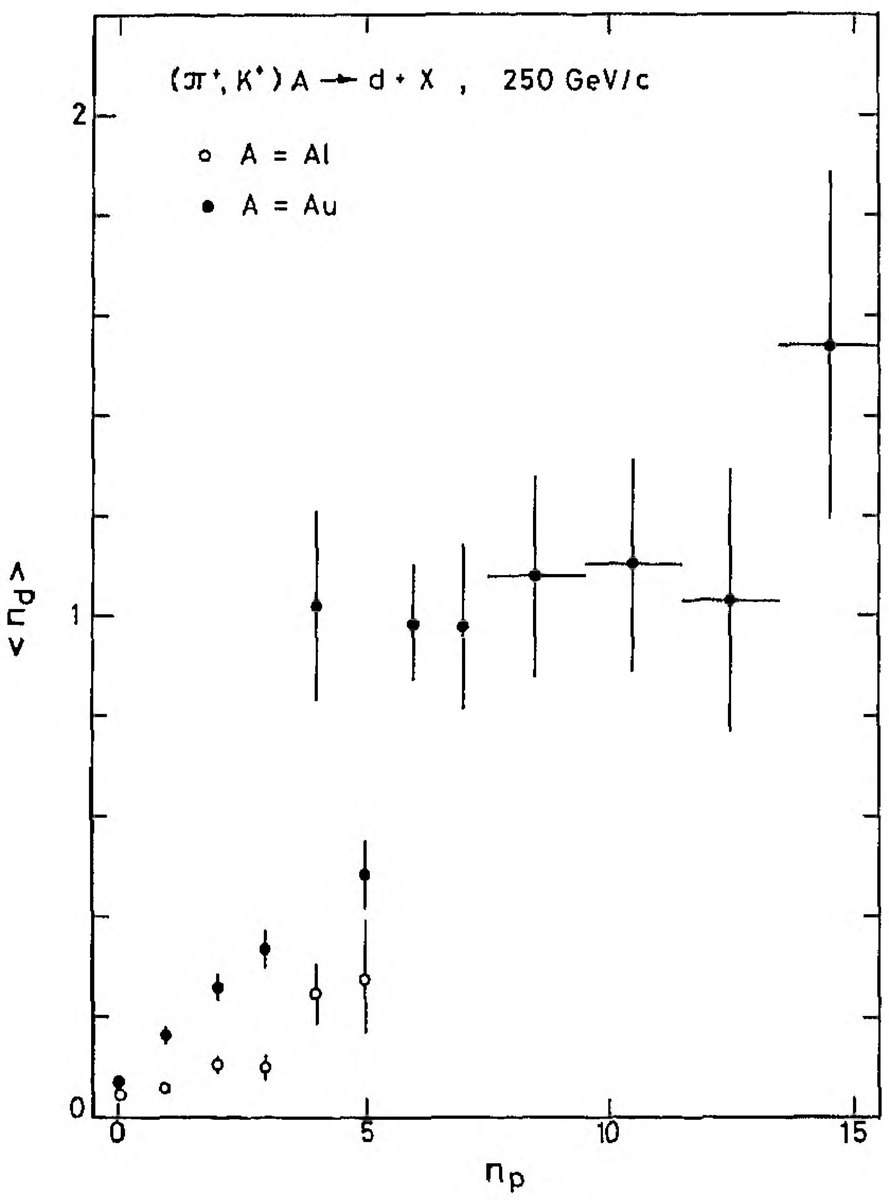

Fig. 8. Mean number of deuterons $\langle n_d \rangle$ as a function of the number of protons

Table 6. Mean proton multiplicity $\langle n_d \rangle$ as a function of charged particle multiplicity n_{ch}

n_{ch}	Al	Au
$1 \div 4$	0.22 ± 0.02	0.23 ± 0.06
$5 \div 9$	0.39 ± 0.02	0.42 ± 0.04
$10 \div 14$	0.58 ± 0.02	0.77 ± 0.04
$15 \div 19$	0.92 ± 0.04	1.19 ± 0.05
$20 \div 24$	1.29 ± 0.06	2.03 ± 0.08
$25 \div 29$	1.76 ± 0.12	2.80 ± 0.11
$30 \div 34$	1.95 ± 0.19	3.65 ± 0.15
$35 \div 39$	1.92 ± 0.35	3.98 ± 0.20
$40 \div 44$	–	4.64 ± 0.25
$45 \div 44$	–	5.26 ± 0.43
$50 \div 54$	–	6.14 ± 0.52
$55 \div 59$	–	6.57 ± 0.50
$60 \div 64$	–	5.20 ± 0.67
$65 \div 69$	–	5.46 ± 0.98

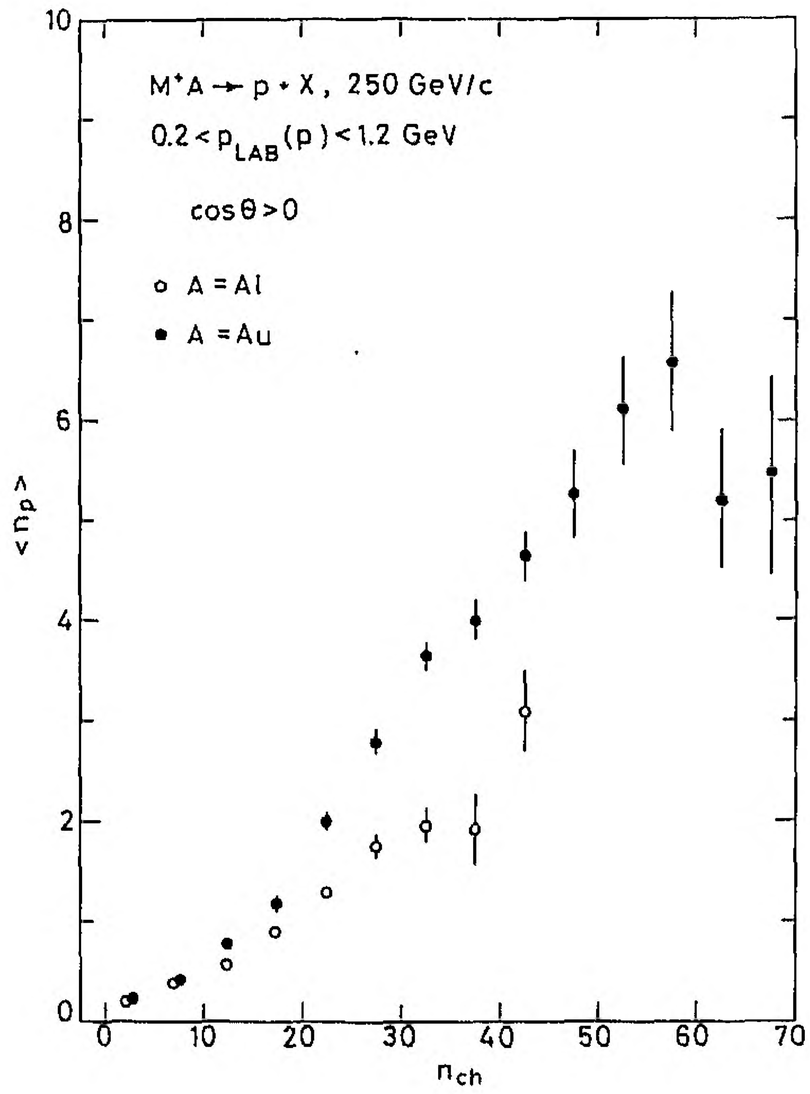

Fig. 9. Mean number of protons $\langle n_d \rangle$ as a function of n_{ch}

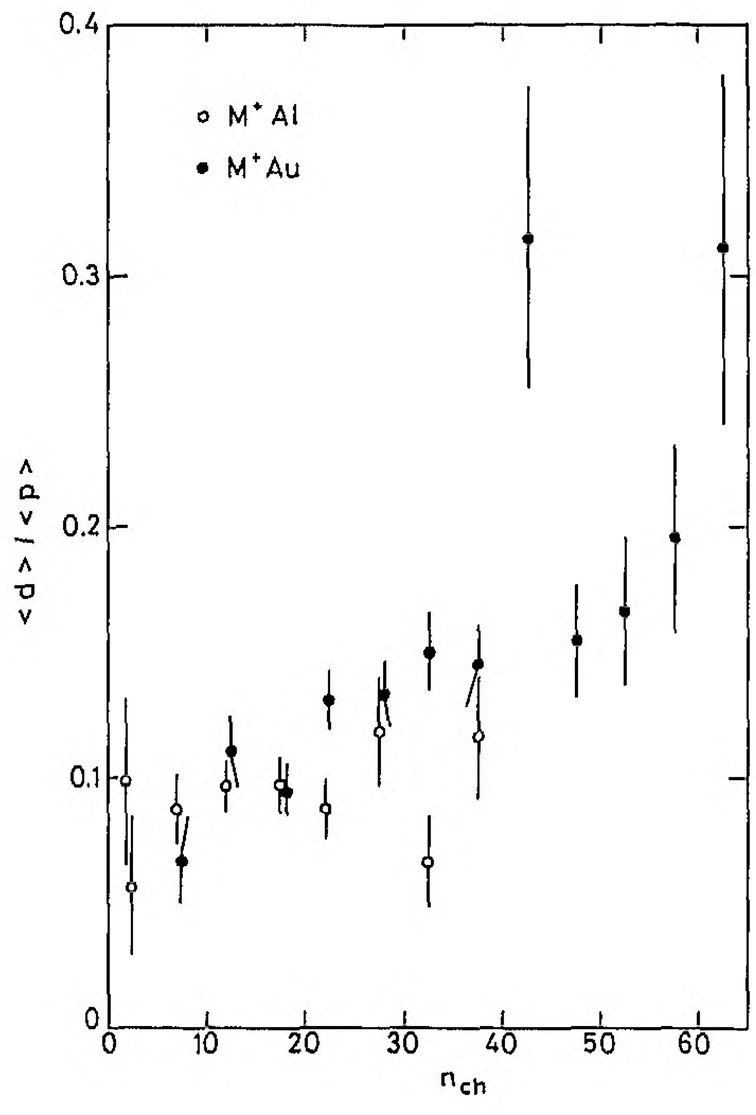

Fig. 10. The ratio of the mean number of deuterons to the mean number of protons, $\langle n_d \rangle / \langle n_p \rangle$, as a function of n_{ch}

The relation between the mean proton multiplicity $\langle n_d \rangle$ and n_{ch} is shown in Fig. 9 and Table 6. This dependence is linear over most of the available interval, with however a quadratic behavior at small n_{ch}. The ratio $\langle n_d \rangle / \langle n_p \rangle$ vs. n_{ch} is shown in Fig. 10. Despite the rather large errors on the data points, the general trends can be summarized as follows:

- for Al, the ratio is almost constant;
- it increases monotonically for Au.

In the limits of statistics, no evidence is observed for a drastic change of the d/p ratio, and therefore no evidence for abrupt entropy change [4]. It is worthwhile to note that an approximate linear dependence of the d/p ratio was also observed in 400 MeV/nucleon Ca + Ca collisions [18] (vs. n_{ch}) and in 450 and 650 MeV/nucleon Nb + Nb collisions [19] (vs. n_p).

4 ($d\pi$) mass spectra

The ($d\pi^-$) effective mass spectrum is shown in Fig. 11 (here and in the following we show unweighted spectra) for the region $0.1 < \beta(d\pi^-) < 0.4$, where $\beta = p/E$ is the velocity of he $d\pi$-system. The lower cut on β practically has no influence on our data, because in this case the deuteron and pion tracks are completely stopped in the target or do not have a sufficient length for momentum measurement from curvature. The upper cut on β eliminates some background in the region of $M(d\pi^-) > 2.3$ GeV. Our resolution in the low mass region is ~ 5 MeV, taking into account both the measurement errors and the uncertainty in the vertex position inside the foil. No evidence for narrow structures is seen.

The ($d\pi^+$) effective mass spectrum for the same cuts is shown in Fig. 12. Also here, no evidence for narrow peaks is observed, nor do we observe a broad enhancement expected at the ΔN threshold ~ 2.15 GeV. If one compares the $d\pi^-$ and $d\pi^+$ mass distributions, an excess of events with $M(d\pi^-) < 2.1$ GeV is noticed.

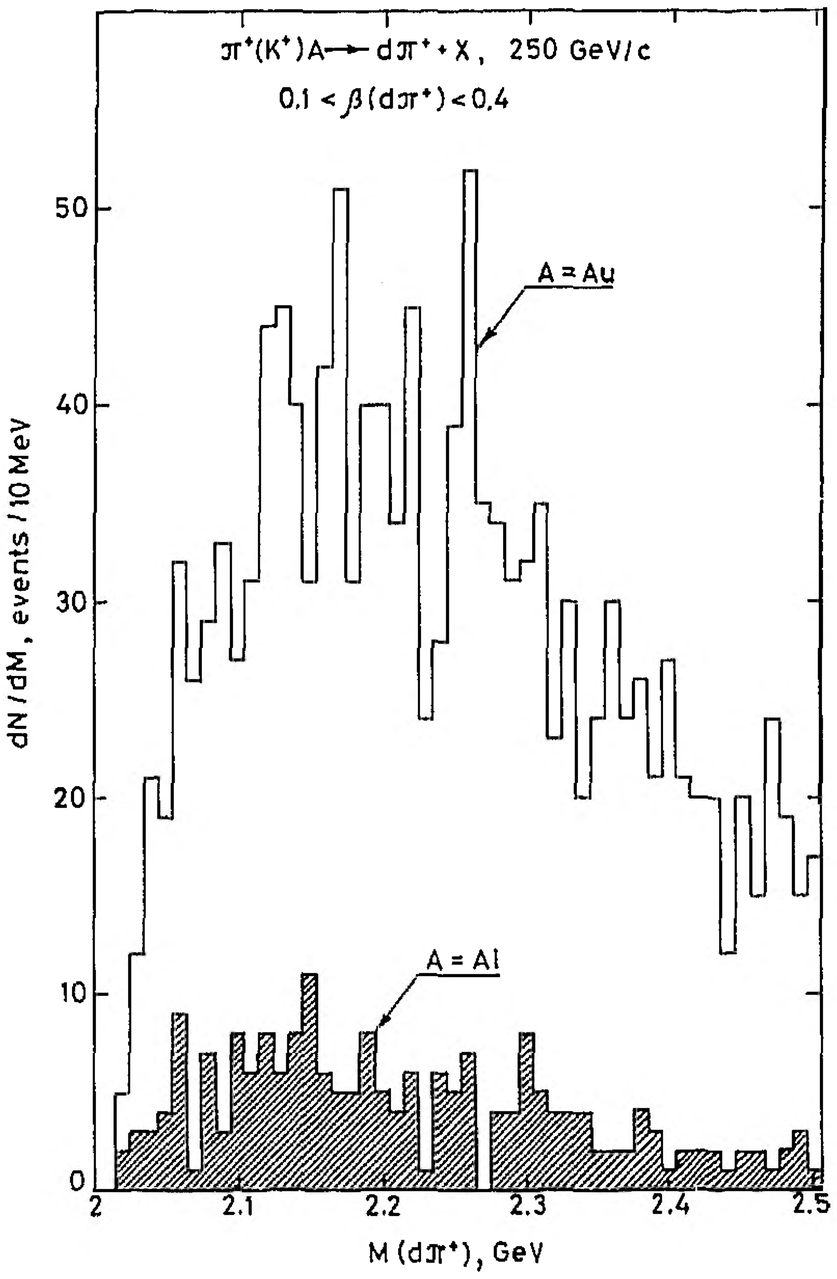

Fig. 12. As in Fig. 11 for $d\pi^+$ combinations

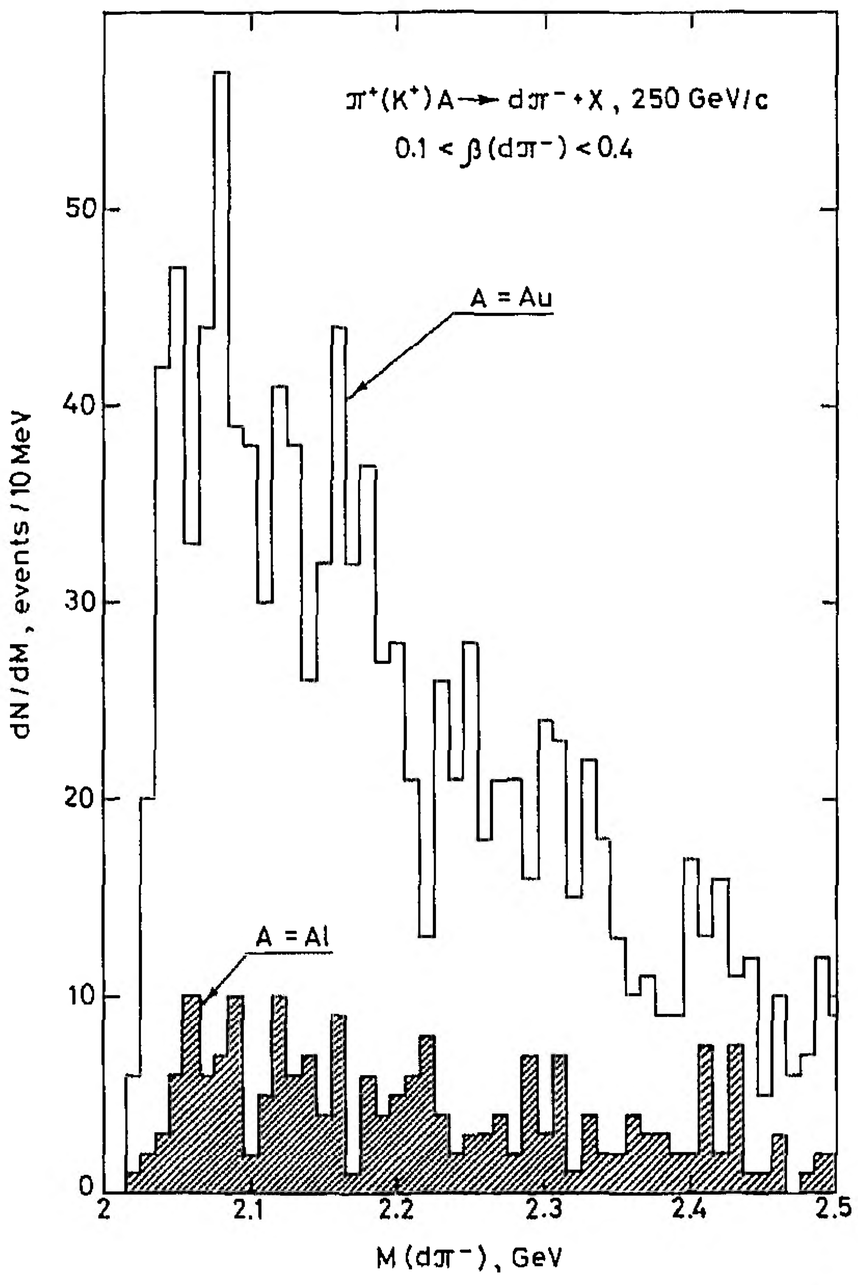

Fig. 11. Distribution of the effective mass $M(d\pi^-)$ for Al and Au targets in the region $0.1 < \beta(d\pi^-) < 0.4$, for events with $n_{ch} < 40$ (Al), < 60 (Au)

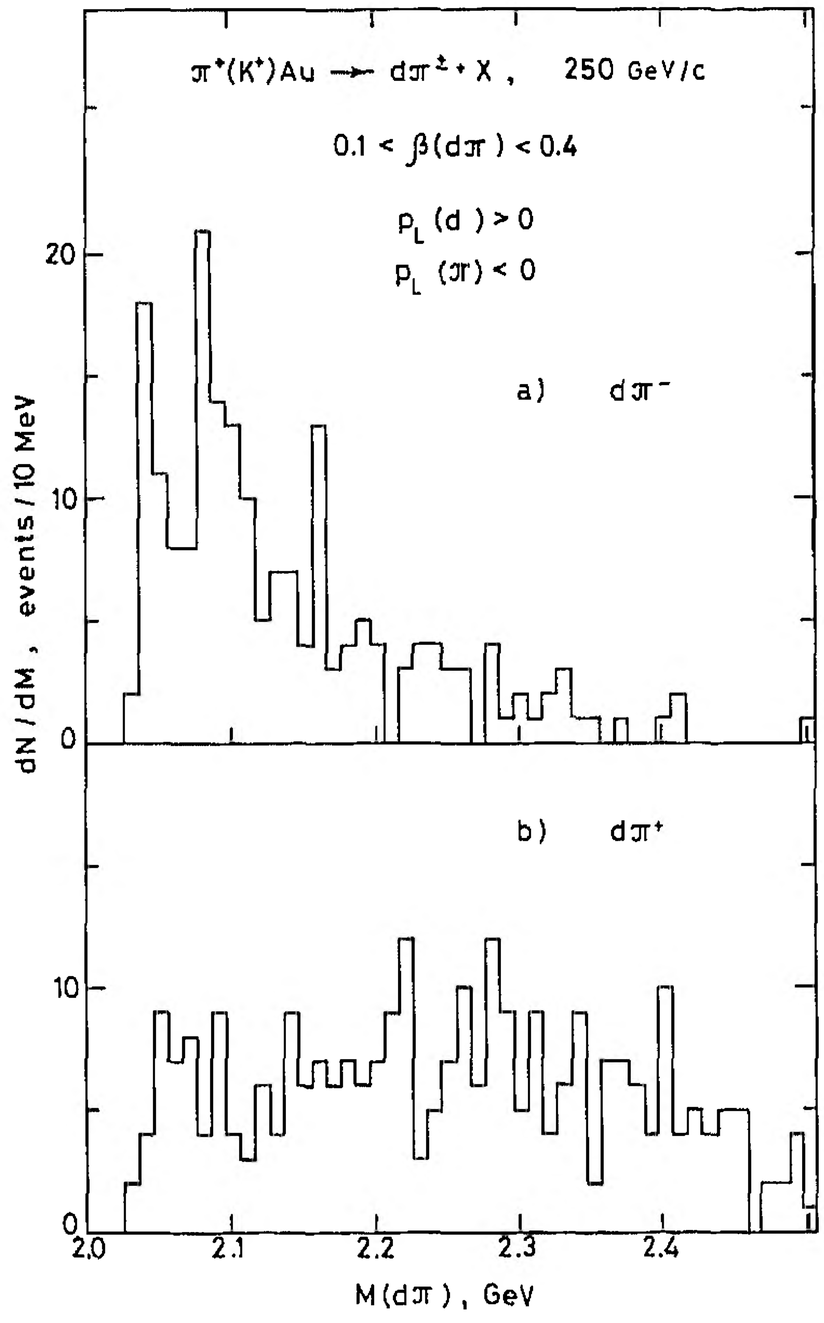

Fig. 13. As in Fig. 11 with the additional cuts on the deuteron and π^- longitudinal momentum components $p_L(d) > 0$, $p_L(\pi^-) < 0$

In our sample of secondary pions, some admixture of electron or positron tracks with $p_{lab} > 0.2$ GeV/c is present since they cannot be identified by ionization. It is therefore necessary to check that this contamination does not generate spikes at low masses. However, unidentified electrons and positrons from γ-conversions and Dalitz-pairs contribute equally to $M(d\pi^-)$ and $M(d\pi^+)$ spectra. The comparison of Fig. 11 and Fig. 12 indicates that this contamination must be small.

Very energetic δ-electrons, produced in the foils from secondary tracks and going forward in the beam direction, may contribute to the $M(d\pi^-)$ spectrum only. To check this, we present the $M(d\pi^-)$ spectrum for the kinematical configuration where the π^- goes backward with respect to the beam direction and the d goes forward (Fig. 13). Some evidence for peaks at $\sim$2.04 and $\sim$2.08 GeV is seen in this figure for the Au sample, corresponding to 3σ signals. The peaks remain at the same level of statistical significance if we request a momentum resolution of the deuteron tracks with $\Delta p/p < 0.1$ i.s.o. 0.3.

5 Summary

We present data on deuteron production at the highest available energy for collisions of positive pions and kaons with Al and Au nuclei. These data can be used e.g. as a reference point in searches of the quark-gluon plasma in collisions of heavy ions. Our main conclusions are the following.

- The average numbers of deuterons found with our selections, amount to 0.071 ± 0.004 in M^+Al and 0.390 ± 0.013 in M^+Au collisions, which is considerably smaller than the corresponding numbers in pAl and pAu collisions [15].
- The fraction of events decreases exponentially with increasing number of deuterons produced. The slope of the exponent is smaller for M^+Au than for M^+Al collisions.
- The $\langle n_d \rangle / \langle n_p \rangle$ ratio as a function of charge multiplicity is constant for M^+Al and increasing for M^+Au collisions.
- We observe narrow peaks in the $M(d\pi^-)$ effective mass spectra at $\sim$2.04 and $\sim$2.08 GeV for the Au sample, however with marginal statistical significance.

Acknowledgments. We would like to thank the scanning and measuring staffs of our laboratories for their careful work and gratefully acknowledge the contribution of the Aachen, Helsinki, Rio, Tbilisi and Warsaw groups for their contributions to the earlier phase of the experiment.

References

1. a. V.B. Gavrilov, G.A. Leksin: Deuteron production in nuclear reactions at high energies. XII ITEP School on Elementary Particles, Moscow, Energoatomizdat, 1985, p. 22 (in Russian);
   b. T. Saniewska, E. Skrypczak, P. Zielinski: Nucl. Phys. 70 (1965) 567;
   c. P. Ciok, M. Soltan, K. Soltynski: Acta Phys. Pol. 4 (1967) 521;
   d. B. Bannik et al.: Yad. Phys. 45 (1987) 431
2. S. Fredriksson, G. Eilam, G. Berlad, L. Bergström: Phys. Rep. 144 (1987) 189
3. L.P. Czernaj, J.I. Kapusta: Phys. Rep. 131 (1986) 224
4. P.J. Siemens, J.I. Kapusta: Phys. Rev. Lett. 43 (1979) 1486
5. a. B. Tatischeff: Nucl. Phys. A446 (1985) 355;
   b. B. Tatischeff et al.: Proc. IX Int. Seminar on high energy physics problems, relativistic nuclear physics and quantum chromodynamics, Dubna 1988, p. 317
6. V.A. Matveev, P. Sorba: Nuovo Cimento 45A (1978) 257
7. Yu.A. Simonov: preprint ITEP-63, 1981, Moscow
8. V.V. Burov et al.: JINR preprint P2-81-621, Dubna, 1981
9. D. Ashery et al.: Phys. Lett. 215B (1989) 41
10. N. Willis et al.: Phys. Lett. 229B (1989) 33
11. L.A. Kondratyuk, B.V. Martemyanov, N.G. Schepkin: Proc. Symposium on Nucleon-Nucleon and Hadron-Nuclear Interactions at Intermediate Energies, Leningrad Institute for Nuclear Physics, Leningrad, 1986, p. 478 (in Russian)
12. M. Adamus et al. (NA22): Z. Phys. C – Particles and Fields 32 (1986) 475
13. a. I.V. Ajinenko et al. (NA22): Z. Phys. C – Particles and Fields 42 (1989) 377;
   b. I.V. Ajinenko et al. (NA22): Z. Phys. C – Particles and Fields 46 (1990) 569
14. I.V. Ajinenko et al.: Z. Phys. C – Particles and Fields 50 (1991) 361
15. J.L. Bailly et al. (NA23): Z. Phys. C – Particles and Fields 35 (1987) 301
16. Particle Data Group: Review of particle properties, Phys. Lett. B204 (1988) 1
17. S.T. Butler, C.A. Pearson: Phys. Rev. 129 (1963) 836
18. H.H. Gutbrod et al.: Phys. Lett. 127B (1983) 317
19. a. K.G.R. Doss et al.: Phys. Rev. C32 (1985) 116;
   b. K.G.R. Doss et al.: Phys. Rev. C37 (1988) 163